ACTA NEUROBIOL. EXP. 1973, 33: 275-286

Lecture delivered at Symposium "Neural control of breathing"
held in Warszawa, August 1971

# ORGANIZATION OF THE PNEUMOTAXIC OSCILLATOR IN THE CAT

A. HUGELIN and F. BERTRAND

Laboratory of Physiology, CHU Saint-Antoine, Paris, France

*Abstract.* The present series concerns the topographical organization of pneumotaxic neurons within the nucleus parabrachialis medialis and adjacent structures according to their respiratory subtype. Results presented were obtained from 1000 units recorded in a region 2.5 mm in height, 1.5 mm in width and 2.5 mm in length. During penetration in the postero-lateral part (mainly in Kölliker-Fuse nucleus) inspiration related cells were found almost exclusively. Phase-spanning inspiratory-expiratory neurons largely predominated in the central core of nucleus parabrachialis medialis. A large majority of expiratory cells was recorded at the antero-medial border of the nucleus. In the intervening regions, clusters of 6 to 10 cells of the inspiratory-expiratory (IE) type alternated with similar clusters of either inspiratory- or expiratory neurons. Phase-spanning expiratory-inspiratory (EI) neurons were mainly found in the intermediary positions between phase-spanning IE and either inspiratory or expiratory columns. A two dimensional reconstruction of pneumotaxic organization is presented and a tentative model of the oscillator is advanced.

The "pneumotaxic centre" was first postulated by Lumsden (1923*ab*). Lumsden observed the apneustic effects of vagal division after transection of the brain stem a few millimeters below the upper limit of the pons. He concluded that there exists a respiratory pacemaker in the most rostral 2 or 3 mm of the pons, which inhibits rhythmically the activity of an "apneustic centre" located in the lower pons (Fig. 1).

A more precise localization of apneusis-producing lesions was attempted by several authors using electrolytic destruction. Pitts, Magoun and Ranson (1939) observed apneusis after coagulation of descending pathways in the ventrolateral part of the mid-pons (Fig. 1); they concluded that there existed a bilateral respiratory structure located in the lateral part of the upper pons. Further studies have localized the pneumotaxic

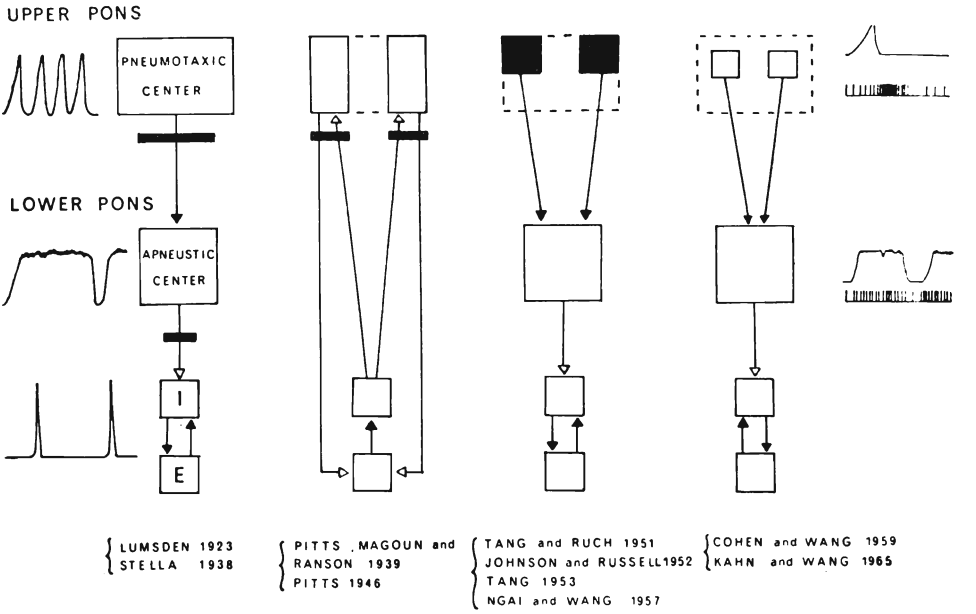


Fig. 1. Schematic representation of the main stages in experimental findings concerning the pneumotaxic centre and ensuing hypotheses. Lesions are represented in black. Explanation in text.

centre in the locus caeruleus (Johnson and Russel 1952), in the extreme dorsolateral part of the anterior pons (Tang and Ruch 1951), in the nucleus dorsalis lemnisci lateralis (Tang 1953), and in the dorsolateral part of the reticular formation (Ngai and Wang 1957). Even though there is no agreement on the exact location of the apneusis-producing area, it should be noticed, however, that in these studies relatively large lesions in the dorsolateral quadrant of the uppermost part of the pons were carried out (Fig. 1).

Cohen and Wang (1959) were the first to call attention to the respiratory function of the nucleus parabrachialis. They observed typical respiratory units in a region including nucleus parabrachialis medialis and lateralis, brachium conjunctivum and locus caeruleus. Cohen and Wang postulated the identity of this respiration-related structure with Lumsden's pneumotaxic centre (Fig. 1).

In a recent series of experiments (Bertrand and Hugelin 1971) we brought forward several observations confirming the localization of the pneumotaxic system in the nucleus parabrachialis medialis (NPBM): (i) cells firing with a respiratory rhythm were found in the NPBM and, as a matter of fact, unit recording gave the impression of an extreme abundance and concentration of respiratory cells (*see also* Dr. Betrand's paper,

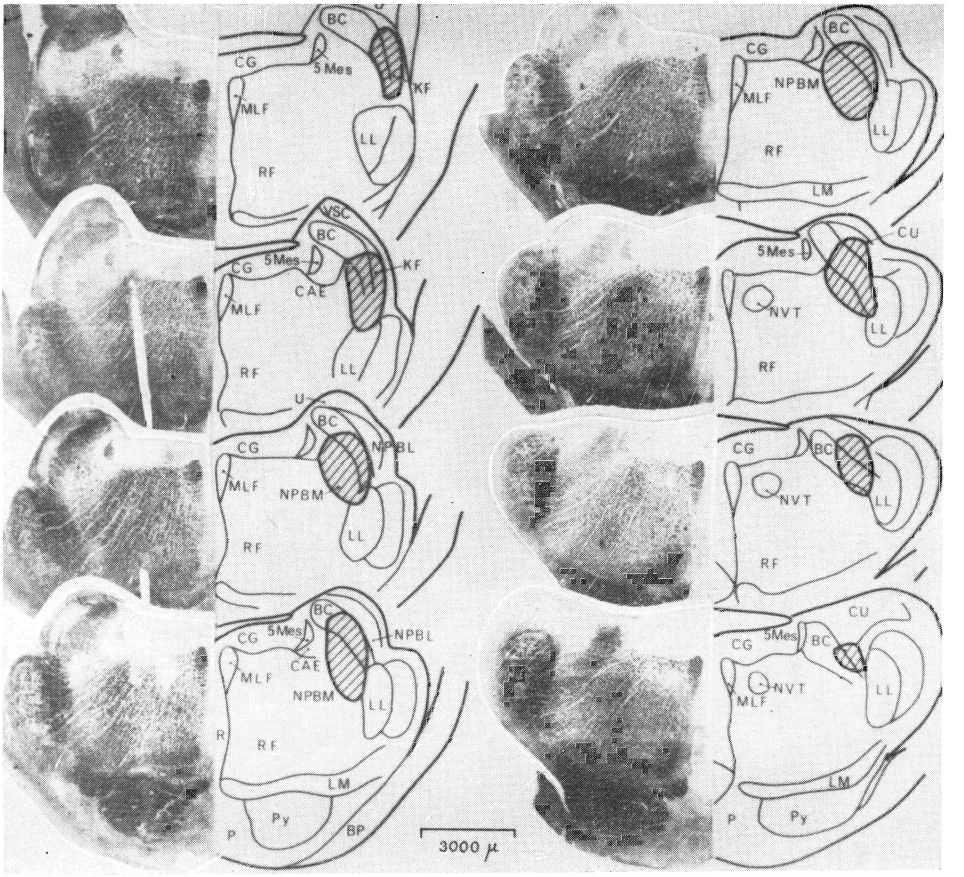


Fig. 3. Anatomical localization of the region from where a large concentration of respiratory units was recorded (striped area). BC, brachium conjunctivum; BP, brachium pontis; CAE, locus caeruleus; CG, griseum centralis; CU, nucleus cuneiformis; KF, Kölliker–Fuse nucleus; LL, lemniscus lateralis; LM, lemniscus medialis; MLF, medial longitudinal fasciculus; NPBL, nucleus parabrachialis lateralis; NPBM, nucleus parabrachialis medialis; NVT, nucleus ventralis tegmenti; P, pontine nuclei; Py, tractus pyramidalis; R, raphé nucleus; RF, reticular formation; U, tractus uncinatus; VSC, ventral spino-cerebellar tract; 5Mes, trigeminal mesencephalic root.

this Symposium). (ii) Unit recording was combined with very restricted electrolytic destruction and it was observed that a lesion as small as 0.25 mm³ (the 1/50 of NPBM volume) produced apneusis, provided it was located in the central core of the nucleus. (iii) Stimulation at points where respiratory units had been just recorded produced powerful effects upon bulbar respiratory neurons. Only two hypotheses can explain these three observations together: (i) NPBM units receive projections from bulbar respiratory neurons and project in turn on bulbar respiratory cells; this is in agreement with the bulbopontine feed-back theory advanced by Pitts (1946), according to which the pneumotaxic system would be a relay in a loop, whose oscillation gives the pace to bulbar respiratory neurons. (ii) NPBM neurons are organized in a more or less complex system of positive and negative feed-back loops, whose efferent discharge would drive periodically bulbar respiratory cells; this is, in some way, like the pacemaker theory advanced by Limsden fifty years ago.

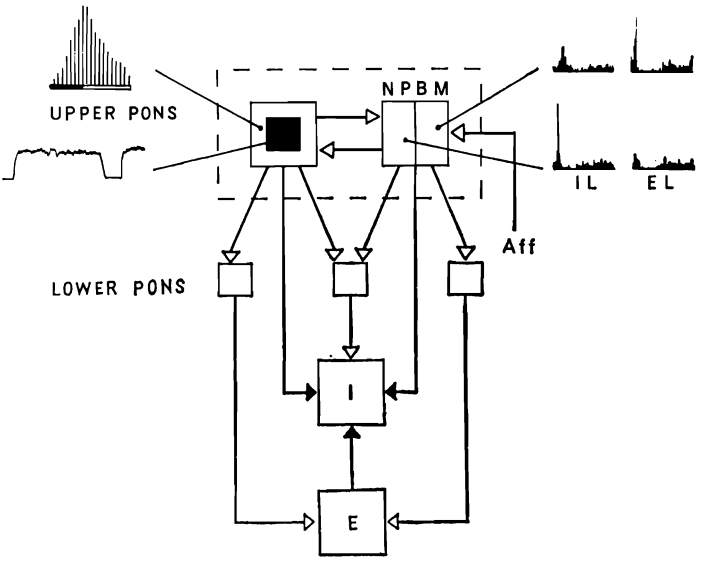


Fig. 2. Summary of previous findings of Bertrand and Hugelin (1971) concerning pneumotaxic localization in the NPBM and its projections to respiratory neurons in lower pons and medulla. Black square represents coagulation in the central core of the NPBM, resulting in apneusis. Unit recording is indicated by the cycle triggered time histogram (left). At right are represented effects of single shock supramaximal stimulation at the antero-medial and postero-lateral part of the NPBM, resulting respectively in an increased probability for immediate onset or cessation of the phrenic burst, as shown in the post-stimulus inspiration latency histogram (IL) and the post-stimulus expiration latency histogram (EL) (right). White arrows indicate excitation, and black, inhibition.

Arguments favouring the last hypothesis were obtained in our series from stimulation experiments. Strong single shocks (1 ma) were delivered through the microelectrode tip at points where respiratory cells had been recorded. It was observed that such excitation had a synchronizing influence on the phrenic burst by resetting the respiratory cycle. Either the onset or cessation of inspiration was avanced (Fig. 2, right, histograms). These results have been explained as effects of stimulation on self-reexciting systems: according to Burns (1956), if a supramaximal single shock is delivered to all the neurons pertaining to a positive feed-back loop, the tonic discharge stops immediately because all the cells pass into the absolute refractory state. Effects of NPBM excitation can be explained in this way: if NPBM excitation falls before the normal time of cessation of the inspiratory phase, a supramaximal excitation of self-reexcitatory inspiratory neurons would bring inspiration to an end and start expiration; likewise if given to self-reexciting expiratory neurons during expiration supramaximal stimulation would stop expiration and advance the onset of next inspiration. These considerations led us to the conclusion that at least two self-reexciting systems are located inside the NPBM, thus supporting the pneumotaxic pacemaker hypothesis. According to the localization of synchronizing points, it was postulated that the inspiratory self-reexciting system is located in the postero-lateral part of the NPBM and the expiratory positive feed-back system in the antero-medial part.

Our research was continued by experiments to be now reported. They concern the topographical organization of respiratory cells within the NPBM according to their firing pattern. Experiments were carried out in the "centre respiratoire isolé" preparation of the cat where the spinal cord is cut at the $C_7$–$T_1$ level and the vagus nerves are sectioned. Recording is performed in unanaesthetized animals immobilized by gallamine perfusion. Care is taken to maintain $PaCO_2$, $PaO_2$, blood pH, arterial blood pressure and central temperature at normal values.

The topography of the region under investigation is presented in Fig. 3. In the left part of each picture a photograph of a histological section of the upper pons is presented. The sections are inclined at a 45° angle to the Horsley–Clarke vertical plane. The interval between sections is 250 $\mu$. At right are outline drawings of nuclei and tracts. The striped areas indicate the region where respiration-related units are densely packed; it comprises the Kölliker–Fuse nucleus, the nucleus parabrachialis medialis and the adjacent portion of brachium conjunctivum and cuneiformis nucleus. The region extends over 2.5 mm in the rostro-caudal direction, 2.5 mm in height and 1.5 mm in width.

In Fig. 4 are presented examples of inspiration triggered histograms

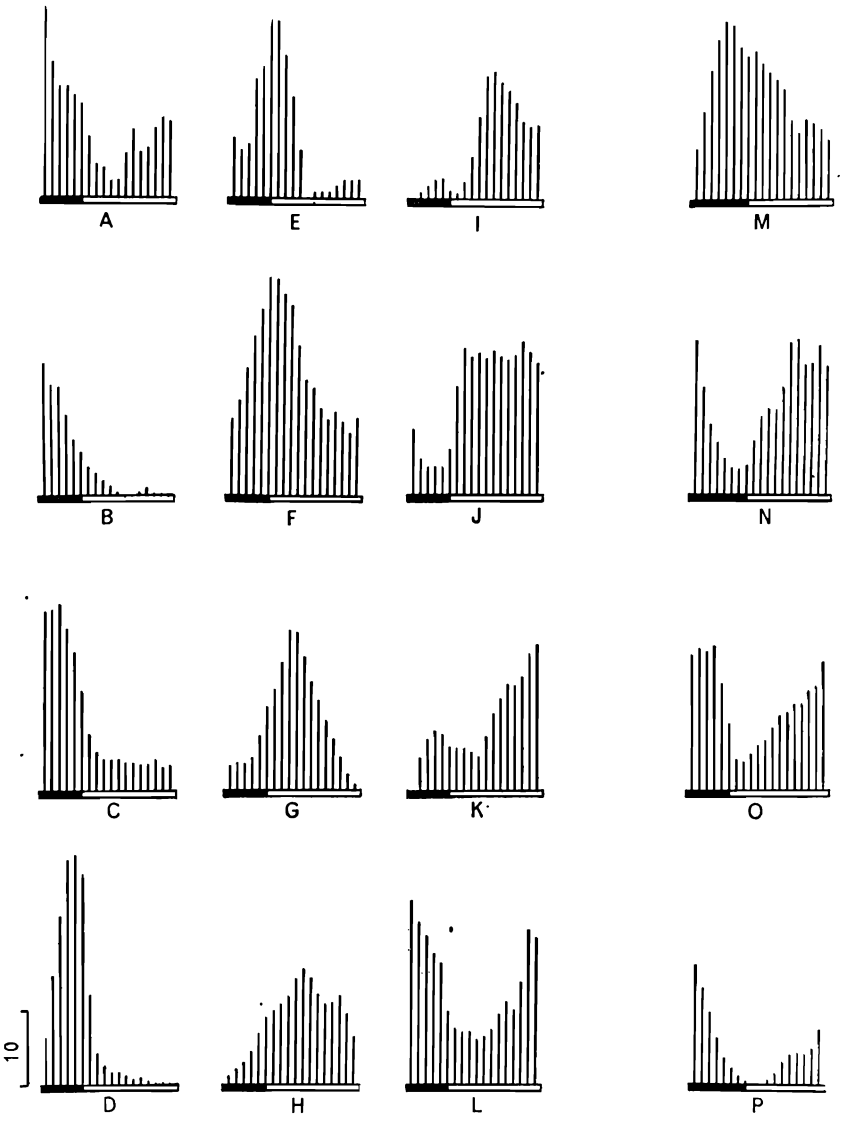


Fig. 4. Cycle triggered histograms of respiratory cells recorded in one individual NPBM. Note the 360° phase shift observed from *A* to *L*. Explanation in text.

obtained from NPBM cells. This method is a variant of poststimulus time histogram; it consists of using the beginning of inspiration to trigger the sequence of bins into which the spikes are distributed. Data processing was carried out on-line, using a PDP-12 digital computer. Histograms of six spikes recorded by two microelectrodes could be computed simultaneously, in addition to histograms of durations of inspiration and total

cycle, and also averaging of phrenic discharge. To avoid smoothing of histograms due to statistical dispersion of phase duration, the programme included rejection of cycles falling outside a predetermined range of duration. In Fig. 4, black and white bars represent inspiration and expiration respectively. It can be first noticed that all units show a tonic discharge. On the other hand they all present an increased frequency during one part of the cycle. Four types of respiratory patterns are seen: (i) inspiratory, (ii) expiratory, (iii) phase-spanning inspiratory-expiratory, and (iv) phase-spanning expiratory-inspiratory (Cohen and Wang 1959, Cohen 1968).

Typical examples of inspiratory firing pattern are shown in *B, C* and *D*. They correspond to several subtypes previously reported at the bulbar level: slowly decreasing in *B*, bell shaped in *C*, and slowly increasing (the most frequent) in *D*. In *I, J* and *K*, the firing rate is higher during expiration. In the phase-spanning inspiratory-expiratory (IE) patterns shown in E to H, the discharge frequency has a maximum near the transition between inspiration and expiration. The phase-spanning expiratory-inspiratory (EI) pattern is presented in *A* and *L;* in this type, the rate of discharge reaches a maximum at the transition between expiration and inspiration.

In experiments of this series, several tens of respiratory cells could be recorded in one NPBM, and the four respiratory patterns were observed to be present simultaneously. It thus appears that the phases of different neurons at the NPBM level occur throughout a range of 360°. This point suggests strongly that circulation of impulses within the NPBM network could explain pneumotaxic oscillation.

Figure 4 illustrates another interesting point. In *M* to *P* are presented histograms from neighboring cells. The *M* histogram is from a large spike and the N histogram from a smaller one recorded through the same microelectrode at the same point. The *M* histogram shows the characteristic IE pattern and the *N* histogram the EI pattern; therefore the two histograms look like mirror images. The *O* and *P* histograms were obtained respectively 80 and 140 $\mu$ deeper in the same penetration; they show a progressive decrease in tonic activity with each neuron; in *P* the discharge stops completely in early expiration. These results could suggest that the low frequency portion of the EI discharge is the result of an inhibitory action exerted by IE neurons.

During NPBM exploration, the four respiratory patterns were found in a definite order related to the lateral and antero-posterior position of the exploring microelectrode. Five characteristic results were obtained. They are shown on Fig. 5. In each column, the drawing at the top represents the anatomical position of the electrode track; the heavy line

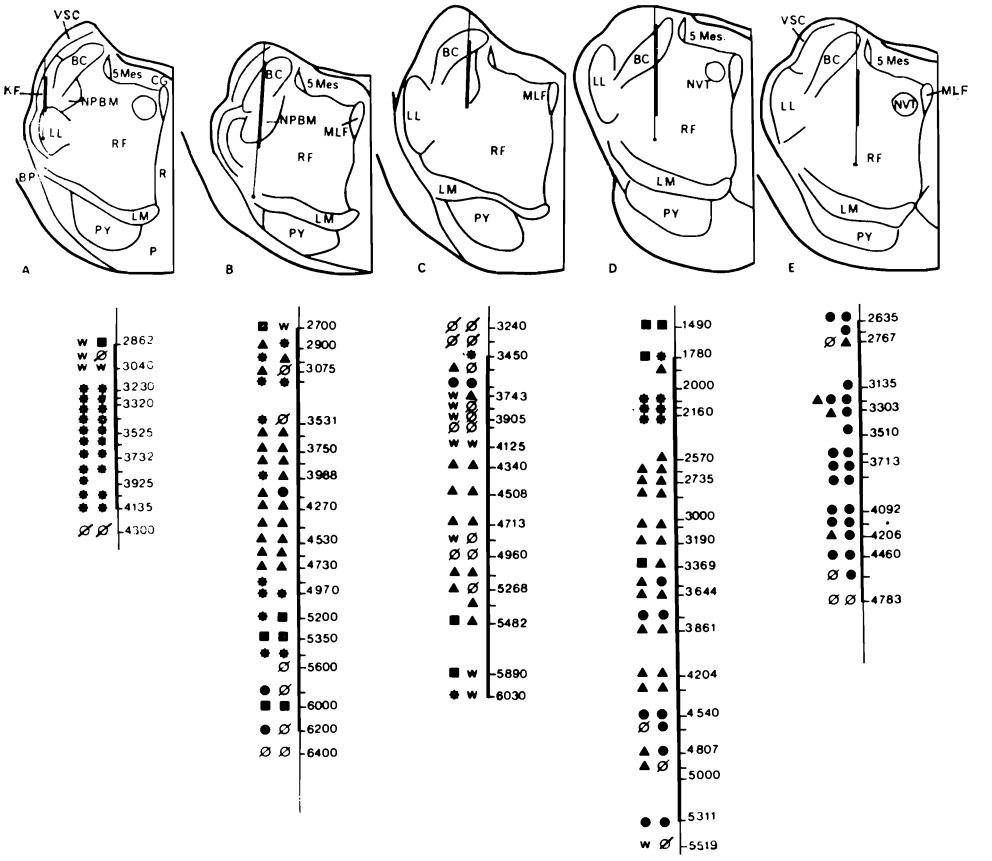


Fig. 5. Results of typical electrode descents in NPBM. Stars, inspiration related neurons; dots, expiration related neurons; triangles, phase-spanning inspiratory-expiratory neurons; squares, phase-spanning expiratory-inspiratory neurons. The numbers at right indicate electrode tip position relative to the $H_0$ Horsley–Clarke reference. For abbreviations *see* Fig. 3.

corresponds to the part of the descent lying in the striped area of Fig. 3. Findings during electrode penetration are reconstructed below, on an enlarged schema of the region of the heavy line; inspiratory cells are represented by stars, expiratory cells by dots, IE neurons by triangles and EI units by squares; the number to the right represents the depth in micron relative to the $H_0$ Horsley-Clarke plane. A particular pattern of distribution was found in each of three different regions: (i) during penetration at the posterolateral part of the NPBM region, mainly in the Kölliker–Fuse nucleus, inspiratory cells were almost exclusively found (Fig. 5*A*); (ii) when the microelectrode was inserted in the central core

of the NPBM, it was observed that IE neurons largely predominated (Fig. 5*C*); (iii) when the electrode was inserted in the most antero-medial part of the NPBM, a large majority of expiratory cells was recorded. In the intervening regions, clusters of 6 to 10 cells firing with the IE respiratory pattern were found over a 300 $\mu$ range on the average; IE clusters alternated with similar clusters of either inspiratory neurons in the intermediary posterior region (Fig. 5*B*), or expiratory units in the intermediary anterior part (Fig. 5*D*). As a matter of fact, microelectrode recording in these intermediary regions gives the impression of successive penetration of folded layers of cells.

Anatomical distribution of EI phase-spanning neurons differs largely from that of the other types: (i) Clusters of EI are never large; they do not exceed 4 to 5 neighbouring neurons recorded within a distance of 100 to 150 $\mu$. (ii) They are diffusely distributed in various parts of the NPBM. (iii) They are mainly found in intermediary positions between phase-spanning IE and expiratory columns. (iv) They predominate in ventral part of the NPBM.

In Fig. 6, a tentative two-dimensional reconstruction of NPBM organization has been attempted. The plane of section crosses the NPBM through its postero-lateral and antero-medial borders. Accordingly three

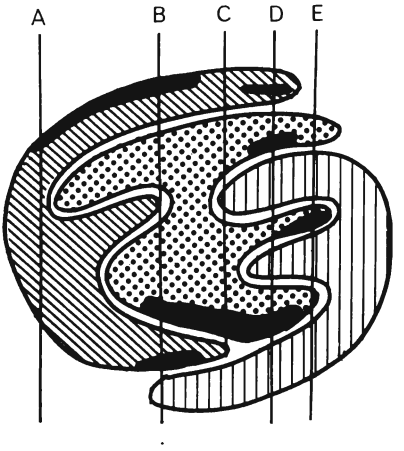


Fig. 6. Two dimensional reconstruction of anatomical distribution of the four subtypes of respiratory neurons in the NPBM. Striped area, inspiration related neurons; vertical lines, expiratory neurons; dotted area, phase -spanning inspiratory-expiratory neurons; black area, phase-spanning expiratory-inspiratory neurons.

vertical columns of neurons are shown: (i) postero-medial for inspiratory neurons, (ii) central for phase-spanning IE neurons, (iii) antero-medial for expiratory neurons. Between them rostrocaudal interdigitations penetrate each other, probably insuring more contacts between the three systems. The phase-spanning EI system is found mainly ventrally but sends widespread extensions towards the inspiratory and expiratory systems.

A tentative model of the pneumotaxic oscillator is presented in Fig. 7. As stated previously, strong stimulation delivered through the microelectrode tip produces a resetting of the respiratory cycle by advancing the next expiration, which is explained by simultaneous excitation of all the neurons pertaining to an inspiratory positive feed-back loop; this effect is obtained by stimulating the postero-lateral part of the NPBM.

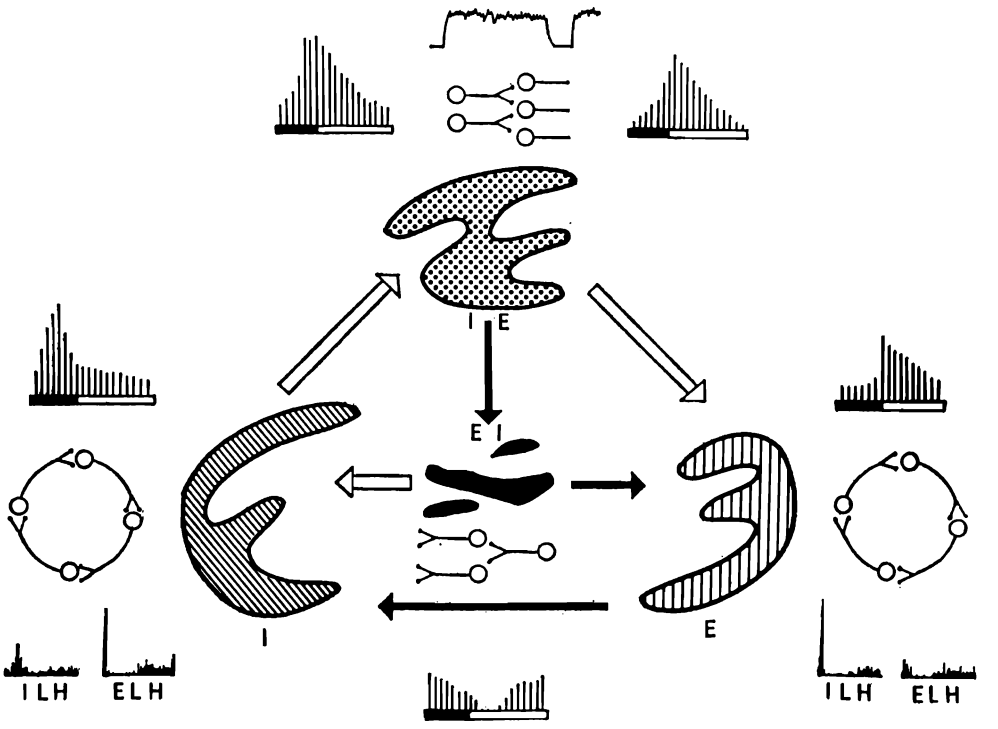


Fig. 7. Tentative model of the pneumotaxic oscillator. Explanation in text.

Localization of inspiratory cells in the same region leads to the conclusion that the inspiratory network located at the postero-lateral region of the NPBM is organized into a self-reexciting system. In the same manner strong stimulation of the antero-medial part of the NPBM produces a resetting of the respiratory cycle by advancing the next inspiration; since this effect is produced by stimulating the antero-medial part of the NPBM in the region where expiratory neurons are recorded, it can be suggested that expiratory neurons are organized as a self-reexciting system.

Connection of neurons in the IE network is probably different: (i) a slow increase in IE unit discharge is observed during inspiration and

a slower decrease during expiration. This effect suggests excitation of IE neurons by inspiratory cells and a persisting excitatory effect when inspiratory discharge stops; (ii) a progressive shift in the peak amplitude of histograms is frequently observed, with anatomical position, in the IE pool from inspiration toward expiration. The peak is more often observed during inspiration in the posterior intermediary region (Fig. 5*B*) and during expiration in the anterior intermediary region (Fig. 5*D*). These two observations suggest a slow transmission of impulses in the IE network and an open chain type of connexion, which would act as a delay system in the transmission of excitation from the inspiratory network to the expiratory subsystem.

As stated above, the EI pattern probably results from and inhibitory action exerted by IE neurons on a tonic discharge. We have no information about internal organization of the EI system but we can postulate that: (i) It stops the expiratory self-reexciting system discharge; this conclusion arises from the finding that EI units are close to expiratory networks and from the progressive decrease of expiratory neuron frequency at the end of expiration at the moment when EI discharge increases (*see* Fig. 4*KL*). (ii) The EI system would excite the inspiratory network, as suggested by the finding of an EI system extending close to it, and also by the observation of some early inspiratory neurons in the postero-lateral region (Fig. 4*B*).

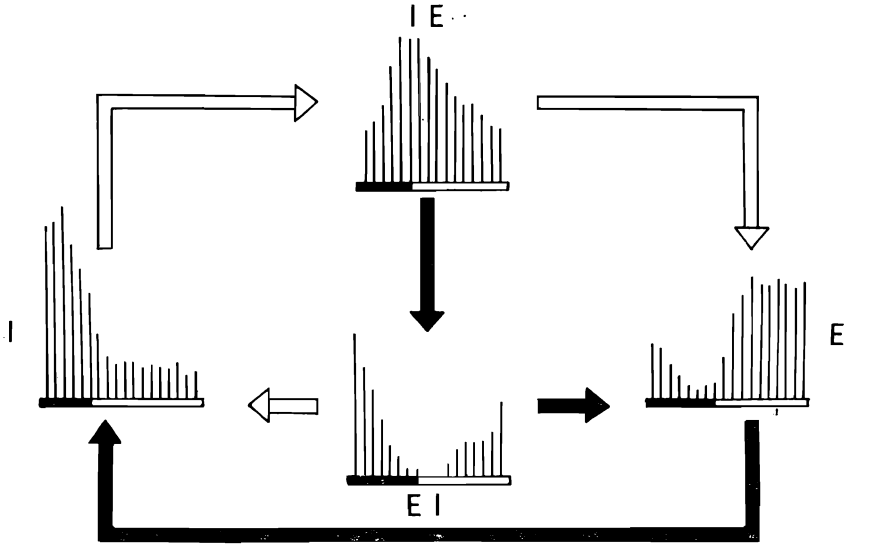


Fig. 8. Summary of the mode of action of the pneumotaxic oscillator. Explanation in text.

Finally, we must postulate a predominating inhibitory influence exerted by the expiratory system upon the inspiratory network to explain the abrupt cessation of inspiration; but, as far as we know, experimental argument favouring this view is lacking.

To summarize (Fig. 8) pneumotaxy, i.e. regular alternation of inspiration and expiration, would result from the interaction of two functional systems at the level of the inspiratory network. The first would comprise excitation of IE neurons by inspiratory system, delayed excitation of expiratory neurons and subsequent immediate inhibition of the inspiratory system. In the second, there takes place delayed excitation of IE neurons, resultant inhibition of EI neurons, subsequent delayed inhibition of expiratory neurons (thus suppressing predominating inhibition on inspiratory neurons) and simultaneous excitation of inspiratory neurons. These two convergent actions on the inspiratory network would trigger the increase of activity in the inspiratory self-reexciting system and start the next inspiration.

This investigation was partially supported by grants from Délégation Générale à la Recherche Scientifique et Technique (66-00-431) and Centre National de la Recherche Scientifique (ERA 233).

## REFERENCES

BERTRAND, F. and HUGELIN, A. 1971. Respiratory synchronizing function of nucleus parabrachialis medialis: pneumotaxic mechanisms. J. Neurophysiol. 34: 189–207.

BERTRAND, F. and VIBERT, J. F. 1973. Distribution of respiratory modulated units in the pons. Acta Neurobiol. Exp. 33: 301–310.

BURNS, B. D. 1956. The cause of reflex afterdischarge in frog's spinal cord. Canad. J. Biochem. 34: 456–465.

COHEN, M. I. 1968. Discharge patterns of brain-stem respiratory neurons in relation to carbon dioxide tension. J. Neurophysiol. 31: 142–165.

COHEN, M. I. and WANG, S. C. 1959. Respiratory neuronal activity in pons of cat. J. Neurophysiol. 22: 33–50.

JOHNSON, F. H. and RUSSELL, G. V. 1952. The Locus coeruleus as a pneumotaxic center. Anat. Record 112: 348. (Abstr.).

LUMSDEN, T. 1923*a*. Observations on the respiratory centres in the cat. J. Physiol. (Lond.) 57: 153–160.

LUMSDEN, T. 1923*b*. Observations on the respiratory centres. J. Physiol. (Lond.) 57: 354–367.

NGAI, S. H. and WANG, S. C. 1957. Organization of central respiratory mechanisms in the brain stem of the cat: localization by stimulation and destruction. Amer. J. Physiol. 190: 343–349.

PITTS, R. F. 1946. Organization of the respiratory center. Physiol. Rev. 26: 609–630.

PITTS, R. F., MAGOUN, H. W. and RANSON, S. W. 1939. The origin of respiratory rhythmicity. Amer. J. Physiol. 127: 654–670.

TANG, P. C. 1953. Localization of the pneumotaxic center in the cat. Amer. J. Physiol. 172: 645–652.

TANG, P. C. and RUCH, T. C. 1951. Localization of the pneumotaxic center in the cat. Amer. J. Physiol. 167: 830–831.

A. HUGELIN and F. BERTRAND, Laboratoire de Physiologie, Centre Hospitalier et Universitaire Saint-Antoine, Paris 12e, 27 rue Chaligny, France.